# Localization of septal accessory pathways using simulated magnetic field maps as templates

R. Hren[1], G. Stroink[2], V. Jazbinsek[1], and Z. Trontelj[1]

*[1]Institute of Mathematics, Physics, and Mechanics, University of Ljubljana, Ljubljana, Slovenia; [2]Department of Physics, Dalhousie University, Halifax, Canada*

## 1 Introduction

Radiofrequency (RF) catheter ablation has become a method of choice in curative treatment of pharmacologically refractory paroxysmal supraventricular tachycardias involving an accessory atrioventricular connection. Prerequisite for successful ablative treatment is the precise identification of an aberrant pathway. Although magnetic field mapping has shown promise in facilitating the localization of preexcitation sites prior to RF intervention (see, e.g., [1]), its ability in discriminating among different septal accessory pathways has yet to be confirmed. The aim of this study is to develop criteria for such discrimination using computer simulations.

## 2 Methods

Our simulation study followed methodology that was presented in detail elsewhere [2,3]. First, we positioned an anatomical model of the human ventricles [3] in the boundary element torso model at the heart's anatomical location documented by radiographic images [3]. Second, we used an anatomical model of the human ventricles [2,3] to simulate the preexcitation sequence. From this realistic sequence, we calculated extracardiac potentials and magnetic field employing the oblique dipole model of cardiac sources [2,3] in combination with the boundary element torso model [3]. Preexcitation sequences were initiated at 12 sites in different regions of the basal septum (see Table 1 and Figure 1). For each sequence, magnetic field maps (MFMs) were calculated at 64 leads above the anterior chest every 2 ms within 40 ms after the onset of preexcitation.

Table 1: *Anatomical description of 10 septal and 2 posterior preexcitation sites.*

| | Abbreviation | Anatomical Description |
|---|---|---|
| 1 | RP | Right posterior |
| 2 | RPP | Right posterior paraseptal |
| 3 | RPP/LPP | |
| 4 | LPP | Left posterior paraseptal |
| 5 | LP | Left posterior |
| 6 | RPP/RIS | |
| 7 | RIS | Right intermediate septal |
| 8 | RIS/RAS | |
| 9 | RAS | Right anterior septal |
| 10 | RAP | Right anterior paraseptal |
| 11 | RAP/LAP | |
| 12 | LAP | Left anterior paraseptal |

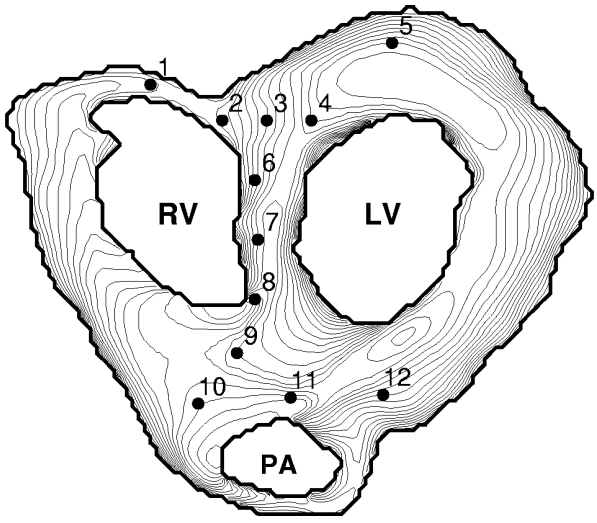


Figure 1: *Basal view of the atrioventricular (AV) ring shown with 12 preexcitation sites. Top 21 layers of the human ventricular model are displayed; they are 1 mm apart, and each is represented by a smoothed contour line to achieve better rendering of the shape. RV, right ventricle; LV, left ventricle; PA, pulmonary artery.*


Figure 2: *MFMs calculated at 16-ms after the onset of activation sequences initiated at 9 septal and two posterior preexcitation sites. The number of a given preexcitation site is shown above each map and corresponds with the site numbering of Figure 1. The extrema are denoted in pT, and isofield lines are plotted for equal intervals, with solid contours representing the magnetic field from the anterior to the posterior torso.*

## 3 Results

Figure 2 shows MFMs calculated at 16 ms after the onset of activation for 9 septal and two posterior preexcitation sites. The morphological changes in MFM patterns were assessed for the preexcitation site at the basal septum in the following order: 1) from the RPP toward RAP regions, 2) from the RAP toward LAP regions, and 3) from the RPP toward LPP regions.

The activation sequence originating at the RPP preexcitation site gives rise to MFMs in which the negative region of the magnetic field (i.e., field vectors pointing from the posterior to the anterior torso) covers the upper anterior torso. Compared to the pattern generated by the activation sequence at the RP preexcitation site, the region of near-zero magnetic field is more vertical and extrema are of lower magnitude. As the preexcitation site is moved closer to the RIS site, the axis joining the extrema rotates clockwise. For MFMs corresponding to the RAP preexcitation site, the positive region of the magnetic field covers the right anterior torso and negative region the left anterior torso.

Comparison between MFMs generated by the activation sequences originating at the RAP and LAP preexcitation sites reveals similar pattern, but in which region of near-zero magnetic field is more vertical for the RAP than LAP site.

For the preexcitation site being shifted from the right-sided septal region toward the left-sided septal region on the posterior side of the epicardium, MFMs feature axis joining the extrema that is progressively rotating clockwise. On the other hand, MFM patterns corresponding to the RP and LP sites are very similar.

The simulated MFMs were visually compared with the maps recorded in patients with WPW syndrome [4-7]. The agreement was good for the right anteroseptal, right anteroparseptal, right posteroparaseptal, left posteroparaseptal and left posterior sites. For some sites (e.g., right anteroparaseptal, left posteroparaseptal sites), simulated and measured maps were difficult to compare because the measured data published in the literature were not consistent (e.g., compare Lamothe et al [5] and Nenonen et al. [7], or Nenonen et al. [1] and Fenici et al. [4].

## 4 Discussion

The use of RF catheter ablation in patients with WPW syndrome requires precise localization of accessory pathways. In particular, precision of RF ablation necessitates distinguishing among anterior, intermediate, and posterior portions of the septum. The simulations presented here suggest that morphological changes in patterns of MFMs could be useful in distinguishing among different septal preexcitation sites, despite that changes in map patterns for some preexcitation sites are subtle. Since we compared the simulated and measured MFMs for only a few preexcitation sites, a comprehensive validation of this simulation study should be carried out.


## Acknowledgements

This work was supported by the Ministry of Science and Technology of Slovenia.


## References


1. J. Nenonen, T. Katila, M. Leiniö, et al., “Magnetocardiographic functional localization using current multipole models’’, *IEEE Trans Biomed Eng* **38,** 648-657, 1991.
2. R. Hren, J. Nenonen, and B.M. Horacek, ``Simulated epicardial potential maps during paced activation reflect myocardial fibrous structure’’, *Ann Biomed Eng* **26,** 1022-1035, 1998.
3. R. Hren, G. Stroink, and B.M. Horacek, ``Spatial resolution of body surface potential maps and magnetic field maps: A simulation study applied to the identification of ventricular preexcitation sites’’, *Med Biol Eng Comp* **36,** 145-157, 1998.
4. R. Fenici, G. Melillo, A. Cappeli, et al., ``Magnetocardiographic localization of Kent bindles’’ in *Advances in Biomagnetism*, S.J. Williamson, M. Hoke, and G. Stroink, Eds. New York: Plenum Press, 1990, pp. 366-368.
5. R. Lamothe, G. Stroink, and M.J. Gardner, ``Body surface potential and magnetic field maps of Wolff-Parkinson-White syndrome patients’’, in *Biomagnetism: fundamental research and clinical applications*, L. Deecke, C. Baumgartner, G. Stroink, and S.J. Williamson, Eds. Amsterdam: Elsevier IOS, 1995, pp. 591-594.
6. M. Mäkijärvi, J. Nenonen, M. Leiniö, et al., ``Localization of accessory pathways in Wolff-Parkinson-White syndrome by high-resolution magnetocardiographic mapping’’, *J Electrocardiol* **25**, 143–155, 1992.
7. J. Nenonen, M. Mäkijärvi, L. Toivonen, et al., “Non-invasive magnetocardiographic localization of ventricular preexcitation in the Wolff-Parkinson-White syndrome using a realistic torso model’’, *Eur Heart J* **14**, 168-174, 1993.